Effect of hyaluronic acid-binding to lipoplexes on intravitreal drug delivery for retinal gene therapy

Thomas F Martens [a,b], Karen Peynshaert [a], Thaís Leite Nascimento [c], Elias Fattal [c], Marcus Karlstetter [d], Thomas Langmann [d], Serge Picaud [e], Jo Demeester [a], Stefaan C De Smedt [a], Katrien Remaut [a], Kevin Braeckmans [a,b,*]

[a] Laboratory of General Biochemistry and Physical Pharmacy, Faculty of Pharmaceutical Sciences, Ghent University, Ottergemsesteenweg 460, 9000 Ghent, Belgium
[b] Center for Nano-and Biophotonics (NB-Photonics), Ghent University, Ottergemsesteenweg 460, 9000 Ghent, Belgium
[c] Univ Paris-Sud, Faculté de Pharmacie, 5, rue J.B. Clément, 92296 Châtenay-Malabry Cedex, France; CNRS UMR 8612, Institut Galien Paris-Sud, 5, rue J.B. Clément, 92296 Châtenay-Malabry Cedex, France.
[d] Department of Ophthalmology, University of Cologne, Cologne, Germany
[e] Institut de la Vision, INSERM, Université Pierre et Marie Curie-Paris 6, 17 rue Moreau, 75 012 Paris, France

*Corresponding author:
Laboratory of General Biochemistry and Physical Pharmacy, Faculty of Pharmaceutical Sciences, Ghent University, Ottergemsesteenweg 460, 9000 Ghent, Belgium
Kevin.Braeckmans@Ugent.be
Tel: +32 9 2648047
Fax: +32 9 2648189

Graphical abstract

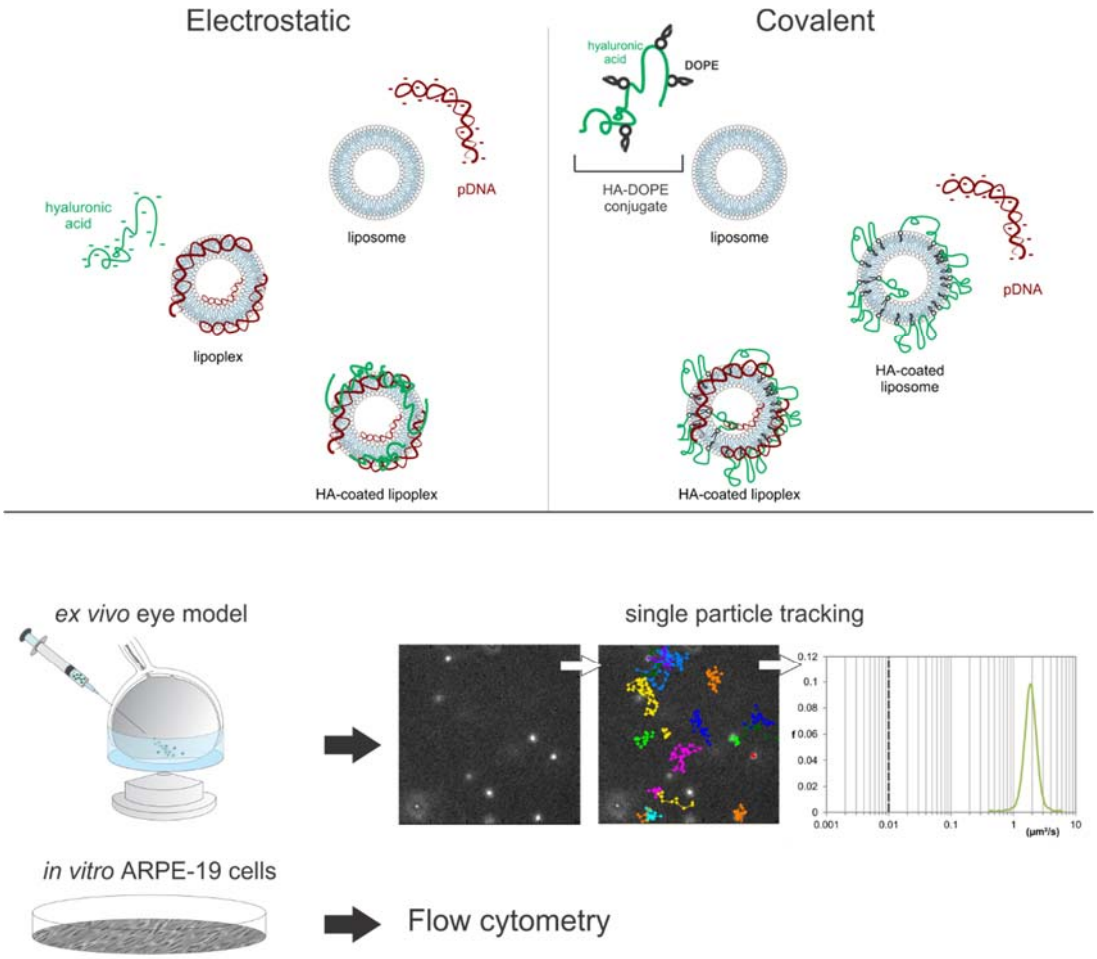

Keywords

hyaluronic acid, lipoplexes, retinal gene therapy, intravitreal administration, nanoparticle mobility

1. Introduction

A wide variety of retinal disorders, often leading to blindness or severely affecting vision, are potential therapeutic targets for retinal gene therapy (Trapani et al., 2014). While most clinical successes have been achieved by subretinal injection of viral vectors, this procedure is very invasive and requires the expertise of vitreoretinal surgeons, limiting its application on a large scale. Due to the local retinal detachment induced during the injection, photoreceptor cell death can occur, resulting in a loss of visual function (Zulliger et al., 2015). In addition, even though viral vectors reach high transfection efficiencies *in vivo*, gene expression is usually limited to the immediate surroundings of the injection site (Igarashi et al., 2013). Furthermore, viral vectors are expensive to produce, and are associated with potential immunogenic reactions and neurotropic dissemination (Kumar-Singh, 2008; Provost et al., 2005). In light of this, intravitreal injection of non-viral vectors could be a more suitable alternative for the delivery of therapeutic nucleic acids (NAs) to the retina.(Adijanto and Naash, 2015) Intravitreal injection of therapeutics is nowadays being performed on a daily basis in the clinic such as for the treatment of wet AMD with anti-VEGF medication like Lucentis®. In contrast to subretinal injection, it can be performed by trained personnel with barely any post-injection complications (Englander et al., 2013). Even though intravitreal injection has been associated with increased ocular pressure (IOP) and a small risk of endophthalmitis, these risks can be easily managed and cannot be compared to the risks of other intraocular administration routes. Furthermore, non-viral vectors offer several advantages over viral vectors, being (i) cheaper to produce on a large scale, (ii) less immunogenic and (iii) higher cargo capacity (Issa and MacLaren, 2012). Especially the latter is important for gene therapy as some hereditary disorders require delivery of a therapeutic gene larger than the cargo capacity of AAV vectors (e.g. ABCA4 for Stargardt syndrome). Typically, non-viral vectors lack the transfection efficiency of their viral counterparts, nor can they bring about stable transfection. Nonetheless, efficient delivery routes could aid in increasing the transfection efficiency of non-viral vectors at the target site.

There is an immense variety of non-viral vectors, differing in composition and surface features. They can be subdivided in two major classes, being polymeric and lipid nanocarriers (Koirala et al., 2013). Both types of nanocarriers usually have a positive charge, which allows them to spontaneously complex with anionic NAs. This results in the formation of spherical particles with sizes ranging around 100 nm to 500 nm with versatile surface characteristics depending on the functionalization of the non-viral vector used (Remaut et al., 2007). We, and others, have previously shown that intravitreally injected nanoparticles can be hampered en route to the retina by the vitreous humor itself. Especially cationic charges and hydrophobicity were shown to be detrimental for intravitreal mobility (Kim et al., 2009; Martens et al., 2013; Peeters et al., 2005; Pitkänen et al., 2003; Xu et al., 2013). We demonstrated that this impaired mobility can be alleviated by surface decoration with polyethylene glycol (PEGylation), though it is also known to be detrimental for cellular interactions (Mishra et al., 2004; Sanders et al., 2007). With the aim to combine optimal vitreal mobility with efficient retinal cell uptake, we have previously proposed to use hyaluronic acid (HA) as an alternative coating strategy for PEG (Martens et al., 2015).

HA is a glycosaminoglycan ubiquitously found in mammals and is a major macromolecular component of the vitreous humor. In recent years, its use in drug delivery has surged due to its biocompatible and non-immunogenic nature, combined with its inherent anionic and viscoelastic properties (Raemdonck et al., 2013). HA molecules have several sites appropriate for chemical modification (e.g. hydroxyl, carboxyl, N-acetyl) which adds to its attractiveness for use in drug delivery. Since HA is a ligand for various cell receptors, most notably CD44, HA-conjugation is abundantly investigated for drug targeting to CD44-overexpressing (tumor) tissues (Arpicco et al., 2013). Also in the field of ocular drug delivery, HA is gaining attention as a drug delivery additive (Apaolaza et al., 2016, 2014; Gan et al., 2013; Koo et al., 2012; Martens et al., 2015). Indeed, we have previously shown that an electrostatic coating of HA was able to increase intravitreal mobility of cationic polymeric gene complexes while maintaining cellular uptake and transfection efficiency (Martens et al., 2015). Also in other recent reports electrostatic HA-coating has been found to improve *in vitro* transfection efficiency of gene

polyplexes in various retinal cell types (Apaolaza et al., 2014; Ruiz De Garibay et al., 2015). However, electrostatic coating of HA may be unstable in contact with extracellular matrices or tissues. It is therefore of interest to evaluate covalent HA coating as a more stable alternative to the electrostatic coating for retinal gene therapy *via* intravitreal administration.

In the present study, we prepared electrostatic and covalent HA-coated lipid gene nanomedicines and compared their performance in terms of vitreal mobility and capacity to transfect retinal cells *in vitro*. Lipid gene nanomedicines containing plasmid DNA (pDNA) were composed of the cationic lipid 1,2-Dioleoyl-3-trimethylammonium-propane (DOTAP) and the fusogenic lipid 1,2-dioleoyl-sn-glycero-3-phosphoethanolamine (DOPE). Intravitreal mobility of both HA-coated lipoplexes was evaluated using our previously published *ex vivo* eye model, using cadaveric bovine eyes and single particle tracking microscopy(Martens et al., 2013). Cellular uptake and transfection was evaluated in an *in vitro* ARPE-19 cell line, representative for the retinal pigment epithelium (RPE) cell layer (Strauss, 2005).

2. Materials and methods

2.1 Materials.

Dulbecco's modified Eagle's medium supplemented with nutrient mixture F12 (DMEM:F12 (1:1), OptiMEM™, Trypan Blue, L-glutamine, fetal bovine serum (FBS), penicillin-streptomycin solution (5000 IU/mL penicillin and 5000 µg/mL streptomycin) (P/S), and Dulbecco's phosphate-buffered saline (DPBS 1x, with or without Ca^{2+}/Mg^{2+}) were supplied by GibcoBRL (Merelbeke, Belgium). 1,2-Dioleoyl-3-trimethylammonium-propane (DOTAP) chloride salt was obtained from Avanti Polar Lipids (Alabaster, AL, USA), 1,2-dioleoyl-sn-glycero-3-phosphoethanolamine (DOPE) from Lipoid GmbH (Ludwigshafen, Germany), 1-ethyl-3-[3-dimethyl)aminopropyl] carbodiimide hydrochloride (EDC) from Sigma-Aldrich (Saint-Quentin Fallavier, France) and high-molecular- weight HA (1,600,000 Da) from Fluka (Sigma-Aldrich Chemie, Buchs, Switzerland). All other reagents were purchased from Sigma-Aldrich (Bornem, Belgium), unless otherwise stated.

2.2 Plasmids.

The plasmid constructs pGL4.13 (4641 bp) and gwiz-GFP (5757 bp) (Promega, Leiden, The Netherlands) were amplified in transformed E. Coli bacteria and isolated from a bacteria suspension with a Purelink™ HiPure Plasmid DNA Gigaprep kit K2100 (Invitrogen, Merelbeke, Belgium). Concentration and purity were determined by UV absorption at 260 nm and 280 nm on a NanoDrop 2000c (Thermo Fisher Scientific, Rockford, IL, USA). Finally, the plasmids were suspended at a concentration of 1 µg/µl and stored in 25 mM HEPES, pH 7.2, at -20°C. For fluorescent labelling of pGL4.13 plasmids with YOYO-1™ (λ_{ex} = 491 nm, λ_{em} = 509 nm, Molecular Probes, Merelbeke, Belgium), YOYO-1 iodide (1 mM in DMSO) was added to the plasmid at a mixing ratio of 0.15:1 (v:w), resulting in a theoretical labelling density of 1 YOYO-dye molecule per 10 base pairs. The mixture was incubated at room temperature for 4 hours in the dark. To remove the DMSO and free YOYO-1, the labelled plasmid was purified with ethanol precipitation and the fluorescently labelled plasmid was finally resuspended in 25 mM HEPES, pH 7.2. The concentration of the plasmid was again determined by UV absorption at 260 nm, and adjusted to 1 µg/µl.

2.3 Conjugation of DOPE to hyaluronic acid.

The HA-DOPE conjugate was synthesized as reported by Surace *et al.* (Surace et al., 2009)based on a modified reaction described by Yerushalmi and Margalit (Yerushalmi and Margalit, 1998). In brief, HA was dissolved in water overnight and preactivated for 2 hours at 37°C by incubation with EDC at pH 4, which was adjusted by titration with 0.1 N HCl. Afterwards, DOPE suspension was added to the HA solution and pH was adjusted to 8.6 with 0.1 M borate buffer. The reaction was allowed to proceed for 24 hours at 37°C. The conjugate was purified by ultrafiltration using a membrane with a molecular weight cut-off of 100000 Da (Amicon Ultrafiltration, Millipore, Billerica, MA). Purity of the conjugate was proven by thin layer chromatography. The successful conjugation was shown by 1H-NMR. The conjugate was lyophilized and stored at -25°C until further use. The coupling degree was determined to be 1.081% w/w (weight DOPE/weight conjugate).

2.4 Liposomes and lipoplexes.

To prepare uncoated liposomes, a thin lipid film was obtained by evaporation under vacuum of a chloroformic solution of an equimolar mixture of DOTAP and DOPE using a rotary vacuum evaporator. This lipid film was rehydrated with 1 ml pure ethanol, for a final molar concentration of 15 mM, and liposomes were further prepared via the ethanol injection method published by Nascimento *et al* (Nascimento et al., 2015). For liposome preparation, 400 µL of ethanolic lipid solution was rapidly injected into 2.6 mL MilliQ water under stirring with a magnetic bar to obtain a final lipid concentration of 2 mM. HA-modified liposomes were prepared by diluting an aqueous stock solution of the HA-DOPE conjugate (1 mg/mL) to different concentrations in MilliQ water before injection of the ethanol-lipid mixture. The content of HA-DOPE conjugate is expressed in percentage molar ratio HA-DOPE/DOTAP lipids (Table 1). For the removal of ethanol, liposome suspensions were dialyzed against distilled water overnight in Slide-A-Lyzer dialysis cassettes with a molecular weight cutoff of 10000 (Thermo Fisher Scientific, Inc., Rockford, IL). Hydrodynamic diameter (intensity-weighted Z-average), polydispersity index (PDI) and zeta potential (ZP) were measured by dynamic light scattering with a NanoZS Zetasizer (Malvern Instruments, Hoeilaart, Belgium). All samples were measured in triplicate, diluted in 25 mM HEPES buffer pH 7.2. The size and zeta potential results for the liposomes can be found in Table 1.

For the preparation of uncoated and PEGylated lipoplexes, a diluted pDNA solution was added to a liposome solution in HEPES buffer at an N/P ratio of 4/1, as described previously (Peeters et al., 2005), with N representing the number of the positive charges (originating from DOTAP) and P the number of the negative charges (originating from the pDNA). This mixture was vortexed for 10 seconds and left to stabilize at room temperature for 15 minutes to allow complexation.

To prepare lipoplexes with a covalent HA-coating (Figure 1 right), a similar protocol was applied where pDNA was added to HA-coated liposomes, while maintaining the N/P ratio of 4/1. Given the concentrations of HA in each liposomes, the resulting lipoplexes had N/P/C ratios ranging from 4/1/0 (uncoated lipoplexes) to 4/1/8 (200 mol% HA-liposomes), where C represent the number of negative

charges originating from the carboxyl-group of the HA-monomer. For the preparation of electrostatically coated HA-lipoplexes, uncoated lipoplexes with the standard 4/1 ratio were prepared. After 15 minutes stabilization, HA diluted in HEPES was added to the lipoplexes corresponding to the previously mentioned N/P/C ratios. These were vortexed for 10 seconds and left to stabilize at room temperature for 15 minutes to allow complexation (Figure 1 left).

2.5 Gel electrophoresis.

Lipoplexes corresponding to 50 ng pDNA were prepared as previously described, after which 5 µl of Ambion loading buffer (Ambion, Merelbeke, Belgium) was added to the suspension. The mixture was loaded on a 1% agarose gel in 1 x TBE buffer, to which GelRed (Biotium, Hayward, CA) was added for visualization of the pDNA. The gel was run for 40 minutes at 100 V and imaged.

2.6 Cell Culture.

ARPE-19 cells (retinal pigment epithelial cell line; ATCC number CRL-2302) were cultured in Dulbecco's modified Eagle's medium supplemented with nutrient mixture F12 (DMEM:F12 (1:1), 10% FBS, 2 mM L-glutamine and 50 µg/ml penicillin/streptomycin). Cells were incubated at 37 °C in a humidified atmosphere containing 5% CO2 and subcultured every 3 to 4 days. Cellular experiments were performed on cells in culture with passage number below 20.

2.7 Uptake and transfection efficiency.

ARPE-19 cells were plated in 24 well plates at 45000 cells/well and allowed to grow overnight. For uptake studies, lipoplexes were prepared the next day with YOYO1-labeled pGL4.13 plasmids as described above, added to the cells in serum-free OptiMEM™ at a concentration of 1 µg pDNA / 45000 cells, and incubated for 2 hours at 37°C in an incubator. As a negative control, ARPE-19 cells were pre-incubated on ice for 1 hour, and also incubated with the particles on ice. After incubation, the particles were removed and ice-cold Trypan Blue was added to each well to quench extracellular fluorescence from lipoplexes attached to the cell membrane. After removal of Trypan Blue, the cells were washed

with DBPS, trypsinized and the green YOYO1-fluorescence from the plasmids in the cell interior was measured by flow cytometry (FACSCalibur™, BD Biosciences Benelux N.V., Erembodegem, Belgium).

For transfection experiments, cells were plated similar to the uptake experiments. The next day, lipoplexes were prepared with gwiz-GFP plasmid to measure transfection efficiency and pGL4.13 plasmid as a negative control, since luciferase expression does not produce a detectable fluorescence signal in GFP-emission spectrum. Incubation of the cells was performed similar to the uptake experiments, where 1 µg pDNA was added to each well and incubated for 2 hours at 37°C. Afterwards, the particles were removed, cells were washed with DPBS and fresh cell culture medium was added for 22 hour incubation. 24 hours after the particles were added, the cells were trypsinized and GFP expression was examined by flow cytometry.

2.8 Flow cytometry.

After inhibition of trypsinization by cell culture medium, cells were centrifuged for 7 minutes at 300 g and supernatant was removed. Cells were resuspended in flow buffer (DPBS / 0,1% sodium azide / 1% bovine serum albumin) and cell-associated fluorescence was analysed with a FACS Calibur (BecktonDickinson, Erembodegem, Belgium) equipped with an Argon laser (excitation 488 nm). For quantification, all experiments were performed in triplicate and for each sample, data was collected for 30 seconds consisting of side scatter, forward scatter and fluorescence emission of YOYO-1 dye (uptake experiments) or GFP (transfection experiments) with a 530/30 nm bandpass filter (FL1). Cellquest software (Beckton Dickinson, Erembodegem, Belgium) was used for analysis. Appropriate gating was applied to the forward/side-scatterplot of untreated cells to select for intact cells. A cell was considered positive for YOYO-1 or GFP fluorescence, if the average fluorescence was above the threshold T, defined as the 99.5 percentile of the negative control sample.

2.9 Cytotoxicity.

Cytotoxicity of the lipoplexes was evaluated with an MTT assay. ARPE-19 cells were plated in 24 well plates at 45000 cells per well. Similar to the transfection protocol, pGL4.13-lipoplexes, prepared as previously described, were added to the cells in serum-free OptiMEM™ and incubated for 2 hour at 37°C. After removal of the particles, fresh cell culture medium was added to the cells and 22 hour afterwards, MTT reagent (with a final concentration of 1 mg/ml) was added to full cell culture medium for 4 hour at 37°C. Finally, cells were washed and lysed with DMSO for 15 minutes on a shaker. Then, absorbance at 590 nm and 690 nm is measured with a plate spectrophotometer (PerkinElmer 2104 EnVision®), where A_{590} relates to the metabolic activity, and A_{690} is used as a reference wavelength.

2.10 Statistical analysis.

Statistical tests were performed in IBM® SPSS® Statistics version 22. Normality of all triplicates was verified with a Shapiro-Wilks test. Average values were further compared by means of an independent samples t-test or Welch's t-test, based on the outcome of the Equality of Variances Levene test. The mean difference was considered significant at the $p < 0.05$ level.

2.11 Ex vivo evaluation of intravitreal lipoplex mobility by single particle tracking microscopy.

Intravitreal mobility of nanoparticles in vitreous humor was evaluated with single particle tracking microscopy in an *ex vivo* model as previously described (Martens et al., 2013). In short, fresh bovine eyes were obtained from a local slaughterhouse, subsequently disposed of extraocular material and incised along the limbus. Then, the cornea and lens were removed, exposing the anterior part of the hyaloid membrane that holds the vitreous body. For all vitreous experiments, the sclera was punctured laterally with a 21 G guard needle (BD Microlance, BD Biosciences Benelux N.V., Erembodegem, Belgium), after which 10-20 µl of nanoparticle suspension was injected in the vitreous humor with the help of a syringe and 25 G spinal needle (BD Microlance, BD Biosciences Benelux N.V., Erembodegem, Belgium). A MatTek glass bottom dish (35 mm, No. 1.5, MatTek Corporation, MA, USA) was positioned against the hyaloid membrane, thus permitting visualization by fluorescence microscopy within the

vitreous humor. The nanoparticles were injected as close as possible to the anterior hyaloid membrane and coverslip to allow visualization within the working distance of the objective lens, though far enough to avoid punctuation of the anterior hyaloid membrane and subsequent outflow of vitreous liquid. Finally, to avoid drift of the eye inside the glass bottom dish, the eye was gently fixed with parafilm. Next, the sample was stored overnight at room temperature before performing the microscopy experiments, thus allowing the nanoparticles to diffuse from the injection site into the surrounding vitreous and within the working range of the objective lens. We have previously observed that the needle used for injection disrupts the fragile vitreal network and forms a cone-like structure (Martens et al., 2013). Nanoparticles were therefore left overnight to diffuse in the surrounding vitreous so that diffusion measurements are performed on nanoparticles in unaffected parts of the vitreous. The microscope was always focused at 5 to 10 µm above the cover slip and for each sample, typically 20 movies of 250 frames each were recorded at different locations within the sample, at a frame rate of 31 fps. All fluorescence video imaging of diffusing nanoparticles was performed on a custom-built laser wide field fluorescence microscope setup. Diffusion analysis of the videos was performed off-line using in-house developed software, as described before (Braeckmans et al., 2010), providing a distribution of apparent diffusion coefficients. For a more detailed description of both the SPT microscope and the trajectory analysis, the reader is referred elsewhere (Martens et al., 2013).

3. Results

3.1 Characterization of HA-coated lipoplexes.

Lipoplexes are composed of anionic pDNA and cationic DOTAP:DOPE liposomes at various molar ratios, with a final layer of anionic HA that is provided as an electrostatic or covalent coating onto the nanoparticle. Uncoated and PEGylated DOTAP:DOPE lipoplexes are also included for comparison at a N/P ratio of 4. Z-average size, polydispersity index and zeta potential of gene lipoplexes is determined with dynamic light scattering (Table 2 and Figure 2). Uncoated lipoplexes are rather monodisperse (PDI <0.3) nanoparticles with a net cationic surface charge. PEGylated lipoplexes have a similar size, while

248 being more monodisperse (PDI = 0.113) and with a more neutral zeta potential due to the shielding of
249 the surface charge by the PEG-chains. Upon coating the cationic lipoplexes with HA, the surface charge
250 of lipoplexes inverts from a positive to a negative charge upon increasing HA-content. Aggregation is
251 observed when the zeta potential becomes near neutral.

252 To verify the complexation efficiency of the HA-coated lipoplexes compared to uncoated lipoplexes,
253 the samples were loaded on a 1% agarose gel (Figure 3). Upon preparing electrostatically coated HA-
254 lipoplexes, no significant decrease in complexation efficiency was noted. For the covalent HA-coated
255 lipoplexes, on the other hand, pDNA complexation appears to be insufficient at those N/P/C-ratios
256 where the HA-coated lipoplexes are not yet colloidally stable (judged by the increased size and PDI for
257 4/1/4-ratios). A bright fluorescent band is visible below the wells, where only little fluorescence is
258 noticeable within the wells. Upon increasing HA-content, pDNA complexation efficiency increases
259 (increase in fluorescence within the well and less fluorescence in the band with free pDNA).

260 **3.2 Intravitreal mobility.**

261 From the characterization results obtained by DLS and gel electrophoresis, we opted to continue with
262 covalent and electrostatic HA-coated lipoplexes with an N/P/C-ratio of 4/1/8 for the following
263 experiments. To evaluate if HA-coating would prevent immobilization in the vitreal matrix, we
264 determined their intravitreal mobility with our previously optimized *ex vivo* eye model (Martens et al.,
265 2013). This model is based on excised bovine eyes from which the anterior segment is removed. By
266 placing a cover slip in the exposed anterior hyaloid membrane, an optical window is created allowing
267 us to visualize movement of nanoparticles in intact vitreous. By using high-resolution fluorescence
268 microscopy and single particle tracking analysis, the intravitreal diffusional mobility profile of a
269 nanoparticle population can be accurately measured. Figure 4 shows the distributions of diffusion
270 coefficients of lipoplexes in the vitreous humor as measured by SPT. First of all, it can be seen that
271 uncoated, cationic lipoplexes show a bimodal diffusion behavior, indicative of a large immobilized
272 fraction. A PEGylation degree of 5% greatly diminishes this immobilization, resulting in a large

population of mobile lipoplexes. Also electrostatic and covalent HA-coating of lipoplexes both show a significant mobility improvement, with covalently coupled HA-lipoplexes giving the best result, likely due to the coating being more stable upon injection into the vitreous humor.

3.3 Uptake and transfection efficiency.

Having determined that both electrostatic and covalent HA-coupling to lipoplexes results in improved intravitreal mobility, it now has to be verified that these nanoparticles can be taken up and transfect retinal target cells. Uptake and transfection efficiencies were determined *in vitro* in an ARPE-19 cell line with flow cytometry. In terms of uptake of YOYO1-labeled lipoplexes (Figure 5A-B), we notice that covalently coated HA-lipoplexes are taken up most efficiently, followed by electrostatic HA-lipoplexes which are taken up to the same extent as uncoated lipoplexes. PEGylation, however, results in significantly less uptake. Interesting to note are the differences in transfection efficiency between the different HA-coated lipoplexes, evaluated by the average amount of GFP expression in the ARPE-19 cell population (Figure 5C-D). First of all, we confirmed that a 5% PEGylation degree significantly decreases the transfection potential of the lipoplexes, resulting in almost no transgene expression. When using an electrostatic coating of HA, no significant differences in transfection efficiency are noted compared to the uncoated lipoplexes, in line with the uptake results (Figure 5D). Remarkably, a covalent coating with HA shows a marked eight-fold increase in transgene expression as compared to uncoated lipoplexes (Figure 5C). Finally, cytotoxicity of all lipoplexes was evaluated with an MTT assay (Figure 5E), from which can be concluded that, even though covalently coupled HA-lipoplexes appear to be slightly more cytotoxic, the HA-lipoplexes are well tolerated by ARPE-19 cells. Taken together we conclude that covalent HA coating of lipoplexes outperforms electrostatic coating, both in terms of intravitreal mobility as its inherent capacity to stimulate its own uptake and transfect ARPE19 cells.

4. Discussion

As retinal gene therapy is advancing in several clinical trials, clinical application might soon become reality. Yet, questions have been raised about the feasibility on a larger scale using current methodologies based on subretinal injection of viral vectors. While intravitreal injection of non-viral gene nanoparticles promises to be less costly and invasive, their therapeutic efficacy to date remains rather low. This can be attributed to the low expression of the transgene in the target cells, though efficient delivery to these target cells after intravitreal injection also poses a major problem. We have previously determined that cationic and hydrophobic surfaces are detrimental to intravitreal mobility of nanoparticles (Martens et al., 2013). By using a PEG-coating, we have shown that nanoparticle mobility in the vitreal matrix can be drastically improved. However, as it is known that PEGylation also decreases cellular interactions and, therefore, uptake and transfection (Mishra et al., 2004; Sanders et al., 2007), we have recently proposed HA as an alternative coating strategy for improved intravitreal mobility while retaining the ability to transfect retinal target cells (Martens et al., 2015). There has been a recent surge in the use of HA in the field of drug delivery due to its inherent biocompatibility and versatile nature (Yadav et al., 2008). There is still an ongoing debate on whether the MW of HA plays a role in the targeting affinity towards hyaladherins (Raemdonck et al., 2013), where some postulate that targeting and uptake efficacy of HA-coated nanoparticles towards CD44-expressing cell types is dependent on the MW of HA (Dufaÿ Wojcicki et al., 2012; Mizrahy et al., 2011), while others have found no such influence of the MW on *in vitro* uptake and transfection efficiency of solid lipid nanoparticles (Ruiz De Garibay et al., 2015). Interestingly, another important factor for CD44 affinity besides MW, has been thought to be grafting density (Qhattal and Liu, 2011), where it is reasoned that the differences in CD44 affinity is due to the way free HA monomers are presented to the hyaladherins. The manner in which HA is coupled to the nanoparticle surface could therefore have an effect on the affinity towards hyaladherins.

In our study, two different approaches of coating lipoplexes with HA were compared in terms of their suitability for intravitreal injection (Figure 1). In the first method, increasing amounts of HA was electrostatically complexed on pre-formed cationic lipoplexes until a negative surface charge was

obtained, indicating successful surface decoration with HA. This is a similar approach as in our previous study where we have electrostatically coated DNA polyplexes with HA (Martens et al., 2015). The second approach entails the random covalent conjugation of DOPE-lipids on the HA polymer, after which liposomes will be formed with an HA-coating attached via insertion of the conjugated DOPE-lipids in the lipid membrane. Covalently coated HA-lipoplexes were formed by complexing nucleic acids with these HA-coated liposomes. By increasing the amount of HA added to the lipoplexes, we determined that both approaches delivered nanosized, monodisperse HA-coated lipoplexes with an anionic surface charge (Figure 2) and capable of incorporating the plasmid DNA (Figure 3).

The first barriers nanoparticles will encounter after intravitreal injection is the vitreous humor itself. We have previously shown that PEGylation could drastically increase the mobility of CBA-ABOL polyplexes and DOTAP:DOPE lipoplexes in the vitreous humor (Martens et al., 2013; Peeters et al., 2005). We further showed that an electrostatic coating of HA on these CBA-ABOL polyplexes also improved intravitreal mobility, especially for HA with low molecular weight (22kDa and 137 kDa) (Martens et al., 2015). In line with these results, in the present study we have found that HA-lipoplexes had markedly increased intravitreal mobility compared to the uncoated lipoplexes. Interesting to note is the bimodal mobility pattern observed for the uncoated lipoplexes, with a large immobilized fraction and a smaller mobile fraction. This is similar to what we have observed before for polyplexes and is likely due to spontaneous electrostatic coating of the lipoplexes with native vitreal HA upon injection. This is supported by the observation that this mobile fraction coincides with the mobile fraction of the electrostatically coated lipoplexes. Nonetheless, covalently coated lipoplexes were slightly more mobile than electrostatically coated ones in the vitreous, approaching the mobility of PEGylated lipoplexes (Figure 4).

We subsequently investigated whether the HA-lipoplexes maintained their ability to transfect retinal target cells compared to uncoated and PEGylated lipoplexes. In this study, ARPE-19 cells were used to verify *in vitro* uptake and transfection efficiency by flow cytometry (Figure 5). Whereas PEGylation

decreased uptake of lipoplexes, electrostatic HA-coated lipoplexes at a 4/1/8-ratio were taken up to the same extent, and covalently coated HA lipoplexes even more than uncoated ones. More importantly, the transgene expression in ARPE-19 cells was nearly eight-fold higher for covalent HA-lipoplexes compared to the uncoated lipoplexes (Figure 5C). Electrostatic HA-lipoplexes, on the other hand, had the same transgene expression as uncoated ones (Figure 5D). We conclude from these experiments that a covalent coupling of HA to the lipoplexes appears to be most beneficial for cellular uptake and subsequent transgene expression. Our results show that the method of HA attachment has a profound influence on the efficacy of HA-coated nanomedicines. Our findings are supported by data from Toriyabe and colleagues (Toriyabe et al., 2011), who noticed that HA-coated liposomes targeted to liver endothelial cells only accumulated at the target site when the HA was covalently attached to the surface of the liposomes, and not when it was present as an electrostatic coating.

These differences between electrostatic and covalent coating could be related to the way that HA monomers are presented to the HA-receptors. Avidity of HA to hyaladherins is dependent on multivalent interactions and several HA-monomers should be available, estimated between 20 and 38, for optimal avidity through divalent binding (Lesley, 2000). Decreased affinity, and possibly decreased cellular uptake, has been proposed to result from a decrease in the degree of freedom the HA molecule experiences when attached to the surface of nanoparticles, thus limiting the amount of potential reaction sites available for binding to the hyaladherins (Mizrahy et al., 2011). Alternatively, the electrostatic coating might be less stable in the complex media used for cell culture, leading to HA polymers detaching from the previously stable nanoparticle. This in turn could result in free HA polymers in the cell culture media competing for the binding sites at cellular hyaladherins, and thus limiting cellular uptake of electrostatic HA-lipoplexes. Covalent HA-lipoplexes, on the other hand, have HA polymers covalently attached to the nanoparticle surface and will be less likely to rearrange in complex media or have HA polymers detaching from the nanoparticle surface. Therefore, it is less likely to have free HA polymers in the cell culture media competing with binding sites of the cellular hyaladherins. Considering the putative differences in avidity between electrostatic and covalent HA-

lipoplexes, and even though uptake of covalent HA-lipoplexes is noticeably higher than that of the electrostatic counterparts, it may not solely account for the eight-fold increase in transgene expression. It could be that the differences in HA presentation and hyaladherins avidity bring about a different entry pathway, and a more efficient subsequent intracellular processing. Indeed, it is a well-known fact that efficiency in transgene expression is not exclusively determined by the amount of cellular uptake, but that different intracellular barriers have to be overcome such as endosomal escape (Martens et al., 2014; Vercauteren et al., 2012). Early studies by Ruponen *et al.* document the influence of extracellular GAGs on transfection efficiency of different non-viral drug delivery systems on smooth muscle cells from rabbit aortic media (Ruponen et al., 2001, 1999). They conclude that differences in transfection efficiency cannot be solely attributed to cellular uptake, and hypothesize that alternative intracellular pathways are likely activated based on the GAGs. Contreras-Ruiz *et al.* also hypothesized in their study that HA influences the uptake pathway and intracellular processing, bypassing the lysosomal pathway and therefore avoiding degradation (Contreras-Ruiz et al., 2011). It could be argued that different coating strategies, and therefore different ways of presenting HA monomers to hyaladherins, would result in different uptake pathways depending on said coating strategies. These are aspects that may be the topic of future studies. Additionally, it is of note that *in vivo*, the RPE cell layer is a highly differentiated cell layer with apicobasal structure. Such differentiation could also bring about changes in extracellular protein expression, with differences in targeting avidity or efficiency for certain ligands. As such, it is of interest to investigate in future studies, the effects of the intracellular processing in differentiated ARPE-19 cells or primary RPE's.

An important aspect that should be kept in mind, is the ability of gene nanotherapeutics to cross the vitreoretinal barrier and permeate the retina towards the RPE cell layer after intravitreal injection. Indeed, the inner limiting membrane is considered to be a potential barrier for nanoparticle penetration in the retina from the vitreous (Dalkara et al., 2009; Puras et al., 2013). Gan and colleagues have shown that core-shell liponanoparticles covalently modified with HA were able to cross the ILM and penetrate the retina (Gan et al., 2013). However they only observed this effect in an experimental

autoimmune uveitis model, while in healthy retinas, the authors found that the nanoparticles remain trapped at the ILM, even up to 7 days after intravitreal injection. A similar observation was made by Iezzi *et al.* for uncoated poly(amido amine) dendrimers (Iezzi et al., 2012). Nevertheless, some studies do show intravitreally injected nanoparticles overcoming the ILM barrier and penetrating into the healthy retina (Bejjani et al., 2005; Bourges et al., 2003; Kim et al., 2009). Most notably, self-assembled amphiphilic polymeric nanoparticles with a 5β-cholanic core and HA-shell were shown to efficiently penetrate the healthy retina of rats 6 hours and 24 hours after intravitreal injection (Koo et al., 2012). The authors further postulated that intravitreal nanoparticles (either with HA-shell or human serum albumin) crossed the ILM by endocytosis in the Müller cells, based on previously published results from this group with human serum albumin-based nanoparticles (Kim et al., 2009). Taken together these variable findings show that further research on this issue is needed, including for the HA coated liposomes presented in this study.

5. Conclusion

In conclusion, we document the differences in behavior of two different approaches for HA-coating of lipoplexes intended for retinal gene therapy *via* intravitreal administration. HA-lipoplexes were prepared either by an electrostatic attachment of HA to preformed lipoplexes, or by the formation of HA-liposomes using a preformed HA-DOPE conjugate. Both approaches resulted in anionic, monodisperse HA-lipoplexes at an N/P/C-ratio of 4/1/8, which markedly improved their intravitreal mobility compared to uncoated lipoplexes in an *ex vivo* vitreal model. Furthermore, we noticed that the HA-lipoplexes were very well tolerated *in vitro* and that transfection efficiency in ARPE-19 cells was not hampered by the HA-coating. On the contrary, a covalent HA-coating provided an eight-fold increase in transgene expression compared to the uncoated and electrostatically coated cationic lipoplexes. Taken together, our data suggest that a covalent coupling of HA to lipoplexes is a promising avenue for gene nanomedicines.

6. Acknowledgements

The ‘Fund for Research in Ophthalmology (FRO)’ and the ‘Stichting voor de blinden (Brailleliga vzw)’ are acknowledged for funding this research. Support by the Ghent University Special Research Fund (BOF) is acknowledged with gratitude.

7. References

Adijanto, J., Naash, M.I., 2015. Nanoparticle-based technologies for retinal gene therapy. Eur. J. Pharm. Biopharm. doi:10.1016/j.ejpb.2014.12.028

Apaolaza, P.S., del Pozo-Rodríguez, A., Solinís, M.A., Rodríguez, J.M., Friedrich, U., Torrecilla, J., Weber, B.H.F., Rodríguez-Gascón, A., 2016. Structural recovery of the retina in a retinoschisin-deficient mouse after gene replacement therapy by solid lipid nanoparticles. Biomaterials 90, 40–49. doi:10.1016/j.biomaterials.2016.03.004

Apaolaza, P.S., Delgado, D., Pozo-Rodríguez, A. Del, Gascón, A.R., Solinís, M.Á., 2014. A novel gene therapy vector based on hyaluronic acid and solid lipid nanoparticles for ocular diseases. Int. J. Pharm. 465, 413–426. doi:10.1016/j.ijpharm.2014.02.038

Arpicco, S., De Rosa, G., Fattal, E., Arpicco, S., De Rosa, G., Fattal, E., 2013. Lipid-Based Nanovectors for Targeting of CD44-Overexpressing Tumor Cells. J. Drug Deliv. 2013, 860780. doi:10.1155/2013/860780

Bejjani, R.A., BenEzra, D., Cohen, H., Rieger, J., Andrieu, C., Jeanny, J.-C., Gollomb, G., Behar-Cohen, F.F., 2005. Nanoparticles for gene delivery to retinal pigment epithelial cells. Mol Vis 11, 124–132.

Bourges, J.L., Gautier, S.E., Delie, F., Bejjani, R. a., Jeanny, J.C., Gurny, R., BenEzra, D., Behar-Cohen, F.F., 2003. Ocular drug delivery targeting the retina and retinal pigment epithelium using polylactide nanoparticles. Investig. Ophthalmol. Vis. Sci. 44, 3562–3569. doi:10.1167/iovs.02-1068

Braeckmans, K., Buyens, K., Bouquet, W., Vervaet, C., Joye, P., Vos, F. De, Plawinski, L., Doeuvre, L., Angles-Cano, E., Sanders, N.N., Demeester, J., Smedt, S.C. De, 2010. Sizing Nanomatter in Biological Fluids by Fluorescence Single Particle Tracking. Nano Lett. 10, 4435–4442.

453 doi:10.1021/nl103264u

454 Contreras-Ruiz, L., de la Fuente, M., Párraga, J.E., López-García, A., Fernández, I., Seijo, B., Sánchez, A.,
455 Calonge, M., Diebold, Y., 2011. Intracellular trafficking of hyaluronic acid-chitosan oligomer-
456 based nanoparticles in cultured human ocular surface cells. Mol. Vis. 17, 279–90.

457 Dalkara, D., Kolstad, K.D., Caporale, N., Visel, M., Klimczak, R.R., Schaffer, D. V, Flannery, J.G., 2009.
458 Inner limiting membrane barriers to AAV-mediated retinal transduction from the vitreous. Mol.
459 Ther. 17, 2096–102. doi:10.1038/mt.2009.181

460 Dufaÿ Wojcicki, A., Hillaireau, H., Nascimento, T.L., Arpicco, S., Taverna, M., Ribes, S., Bourge, M.,
461 Nicolas, V., Bochot, A., Vauthier, C., Tsapis, N., Fattal, E., 2012. Hyaluronic acid-bearing lipoplexes:
462 Physico-chemical characterization and in vitro targeting of the CD44 receptor. J. Control. Release
463 162, 545–552. doi:10.1016/j.jconrel.2012.07.015

464 Englander, M., Chen, T.C., Paschalis, E.I., Miller, J.W., Kim, I.K., 2013. Intravitreal injections at the
465 Massachusetts Eye and Ear Infirmary: analysis of treatment indications and postinjection
466 endophthalmitis rates. Br. J. Ophthalmol. 97, 460–5. doi:10.1136/bjophthalmol-2012-302435

467 Gan, L., Wang, J., Zhao, Y., Chen, D., Zhu, C., Liu, J., Gan, Y., 2013. Hyaluronan-modified core-shell
468 liponanoparticles targeting CD44-positive retinal pigment epithelium cells via intravitreal
469 injection. Biomaterials 34, 5978–5987. doi:10.1016/j.biomaterials.2013.04.035

470 Iezzi, R., Guru, B.R., Glybina, I. V., Mishra, M.K., Kennedy, A., Kannan, R.M., 2012. Dendrimer-based
471 targeted intravitreal therapy for sustained attenuation of neuroinflammation in retinal
472 degeneration. Biomaterials 33, 979–988. doi:10.1016/j.biomaterials.2011.10.010

473 Igarashi, T., Miyake, K., Asakawa, N., Miyake, N., Shimada, T., Takahashi, H., 2013. Direct comparison
474 of administration routes for AAV8-mediated ocular gene therapy. Curr. Eye Res. 38, 569–77.
475 doi:10.3109/02713683.2013.779720

476 Issa, P.C., MacLaren, R.E., 2012. Non-viral retinal gene therapy: a review. Clin. Experiment. Ophthalmol.
477 40, 39–47. doi:10.1111/j.1442-9071.2011.02649.x

478 Kim, H., Robinson, S.B., Csaky, K.G., 2009. Investigating the movement of intravitreal human serum
479 albumin nanoparticles in the vitreous and retina. Pharm. Res. 26, 329–337. doi:10.1007/s11095-
480 008-9745-6

481 Koirala, A., Conley, S.M., Naash, M.I., 2013. A review of therapeutic prospects of non-viral gene therapy
482 in the retinal pigment epithelium. Biomaterials 34, 7158–7167.
483 doi:10.1016/j.biomaterials.2013.06.002

484 Koo, H., Moon, H., Han, H., Na, J.H., Huh, M.S., Park, J.H., Woo, S.J., Park, K.H., Kwon, I.C., Kim, K., Kim,
485 H., 2012. The movement of self-assembled amphiphilic polymeric nanoparticles in the vitreous
486 and retina after intravitreal injection. Biomaterials 33, 3485–93.
487 doi:10.1016/j.biomaterials.2012.01.030

488 Kumar-Singh, R., 2008. Barriers for retinal gene therapy: Separating fact from fiction. Vision Res. 48,
489 1671–1680. doi:10.1016/j.visres.2008.05.005

490 Lesley, J., 2000. Hyaluronan Binding by Cell Surface CD44. J. Biol. Chem. doi:10.1074/jbc.M002527200

491 Martens, T.F., Remaut, K., Demeester, J., De Smedt, S.C., Braeckmans, K., 2014. Intracellular delivery
492 of nanomaterials: How to catch endosomal escape in the act. Nano Today 9, 344–364.
493 doi:10.1016/j.nantod.2014.04.011

494 Martens, T.F., Remaut, K., Deschout, H., Engbersen, J.F.J., Hennink, W.E., Van Steenbergen, M.J.,
495 Demeester, J., De Smedt, S.C., Braeckmans, K., 2015. Coating nanocarriers with hyaluronic acid
496 facilitates intravitreal drug delivery for retinal gene therapy. J. Control. Release 202, 83–92.
497 doi:10.1016/j.jconrel.2015.01.030

498 Martens, T.F., Vercauteren, D., Forier, K., Deschout, H., Remaut, K., Paesen, R., Ameloot, M.,
499 Engbersen, J.F., Demeester, J., De Smedt, S.C., Braeckmans, K., 2013. Measuring the intravitreal
500 mobility of nanomedicines with single-particle tracking microscopy. Nanomedicine 8, 1955–1968.
501 doi:10.2217/nnm.12.202

502 Mishra, S., Webster, P., Davis, M.E., 2004. PEGylation significantly affects cellular uptake and
503 intracellular trafficking of non-viral gene delivery particles. Eur. J. Cell Biol. 83, 97–111.
504 doi:10.1078/0171-9335-00363

505 Mizrahy, S., Raz, S.R., Hasgaard, M., Liu, H., Soffer-Tsur, N., Cohen, K., Dvash, R., Landsman-Milo, D.,
506 Bremer, M.G.E.G., Moghimi, S.M., Peer, D., 2011. Hyaluronan-coated nanoparticles: The
507 influence of the molecular weight on CD44-hyaluronan interactions and on the immune
508 response. J. Control. Release 156, 231–238. doi:10.1016/j.jconrel.2011.06.031

509 Nascimento, T.L., Hillaireau, H., Noiray, M., Bourgaux, C., Arpicco, S., Pehau-Arnaudet, G., Taverna, M.,
510 Cosco, D., Tsapis, N., Fattal, E., 2015. Supramolecular Organization and siRNA Binding of
511 Hyaluronic Acid-Coated Lipoplexes for Targeted Delivery to the CD44 Receptor. Langmuir 31,
512 11186–11194. doi:10.1021/acs.langmuir.5b01979

513 Peeters, L., Sanders, N.N., Braeckmans, K., Boussery, K., Van De Voorde, J., De Smedt, S.C., Demeester,
514 J., 2005. Vitreous: A barrier to nonviral ocular gene therapy. Investig. Ophthalmol. Vis. Sci. 46,
515 3553–3561. doi:10.1167/iovs.05-0165

516 Pitkänen, L., Ruponen, M., Nieminen, J., Urtti, A., 2003. Vitreous is a barrier in nonviral gene transfer
517 by cationic lipids and polymers. Pharm. Res. 20, 576–583. doi:10.1023/A:1023238530504

518 Provost, N., Lemeur, G., Weber, M., Mendesmadeira, A., Podevin, G., Cherel, Y., Colle, M., Deschamps,
519 J., Moullier, P., Rolling, F., 2005. Biodistribution of rAAV Vectors Following Intraocular
520 Administration: Evidence for the Presence and Persistence of Vector DNA in the Optic Nerve and

521 in the Brain. Mol. Ther. 11, 275–283. doi:10.1016/j.ymthe.2004.09.022

522 Puras, G., Zarate, J., Aceves, M., Murua, A., Díaz, A.R., Avilés-Triguero, M., Fernández, E., Pedraz, J.L.,
523 2013. Low molecular weight oligochitosans for non-viral retinal gene therapy. Eur. J. Pharm.
524 Biopharm. 83, 131–140. doi:10.1016/j.ejpb.2012.09.010

525 Qhattal, H.S.S., Liu, X., 2011. Characterization of CD44-Mediated Cancer Cell Uptake and Intracellular
526 Distribution of Hyaluronan-Grafted Liposomes. Mol. Pharm. 8, 1233–1246.
527 doi:10.1021/mp2000428

528 Raemdonck, K., Martens, T.F., Braeckmans, K., Demeester, J., De Smedt, S.C., 2013. Polysaccharide-
529 based nucleic acid nanoformulations. Adv. Drug Deliv. Rev. 65, 1123–1147.
530 doi:10.1016/j.addr.2013.05.002

531 Remaut, K., Sanders, N.N., De Geest, B.G., Braeckmans, K., Demeester, J., De Smedt, S.C., 2007. Nucleic
532 acid delivery: Where material sciences and bio-sciences meet. Mater. Sci. Eng. R Reports.
533 doi:10.1016/j.mser.2007.06.001

534 Ruiz De Garibay, A.P., Solinís, M.A., Del Pozo-Rodríguez, A., Apaolaza, P.S., Shen, J.S., Rodríguez-
535 Gascón, A., 2015. Solid lipid nanoparticles as non-viral vectors for gene transfection in a cell
536 model of fabry disease. J. Biomed. Nanotechnol. 11, 500–511. doi:10.1166/jbn.2015.1968

537 Ruponen, M., Rönkkö, S., Honkakoski, P., Pelkonen, J., Tammi, M., Urtti, A., 2001. Extracellular
538 Glycosaminoglycans Modify Cellular Trafficking of Lipoplexes and Polyplexes. J. Biol. Chem. 276,
539 33875–33880. doi:10.1074/jbc.M011553200

540 Ruponen, M., Ylä-Herttuala, S., Urtti, A., 1999. Interactions of polymeric and liposomal gene delivery
541 systems with extracellular glycosaminoglycans: Physicochemical and transfection studies.
542 Biochim. Biophys. Acta - Biomembr. 1415, 331–341. doi:10.1016/S0005-2736(98)00199-0

543 Sanders, N.N., Peeters, L., Lentacker, I., Demeester, J., De Smedt, S.C., 2007. Wanted and unwanted
544 properties of surface PEGylated nucleic acid nanoparticles in ocular gene transfer. J. Control.
545 Release 122, 226–235. doi:10.1016/j.jconrel.2007.05.004

546 Strauss, O., 2005. The Retinal Pigment Epithelium in Visual Function. Physiol. Rev. 85, 845–881.
547 doi:10.1152/physrev.00021.2004

548 Surace, C., Arpicco, S., Dufaÿ-Wojcicki, A., Marsaud, V., Bouclier, C., Clay, D., Cattel, L., Renoir, J.-M.,
549 Fattal, E., 2009. Lipoplexes targeting the CD44 hyaluronic acid receptor for efficient transfection
550 of breast cancer cells. Mol. Pharm. 6, 1062–73. doi:10.1021/mp800215d

551 Toriyabe, N., Hayashi, Y., Hyodo, M., Harashima, H., 2011. Synthesis and evaluation of stearylated
552 hyaluronic acid for the active delivery of liposomes to liver endothelial cells. Biol. Pharm. Bull. 34,
553 1084–9.

554 Trapani, I., Puppo, A., Auricchio, A., 2014. Vector platforms for gene therapy of inherited retinopathies.
555 Prog. Retin. Eye Res. 43, 108–128. doi:10.1016/j.preteyeres.2014.08.001

556 Vercauteren, D., Rejman, J., Martens, T.F., Demeester, J., De Smedt, S.C., Braeckmans, K., 2012. On the
557 cellular processing of non-viral nanomedicines for nucleic acid delivery: Mechanisms and
558 methods. J. Control. Release 161, 566–581. doi:10.1016/j.jconrel.2012.05.020

559 Xu, Q., Boylan, N.J., Suk, J.S., Wang, Y.-Y., Nance, E.A., Yang, J.-C., McDonnell, P.J., Cone, R.A., Duh, E.J.,
560 Hanes, J., 2013. Nanoparticle diffusion in, and microrheology of, the bovine vitreous ex vivo. J.
561 Control. Release 167, 76–84. doi:10.1016/j.jconrel.2013.01.018

562 Yadav, A.K., Mishra, P., Agrawal, G.P., 2008. An insight on hyaluronic acid in drug targeting and drug
563 delivery. J. Drug Target. 16, 91–107. doi:10.1080/10611860802095494

564 Yerushalmi, N., Margalit, R., 1998. Hyaluronic Acid-Modified Bioadhesive Liposomes as Local Drug

565 Depots: Effects of Cellular and Fluid Dynamics on Liposome Retention at Target Sites. Arch.
566 Biochem. Biophys. 349, 21–26. doi:10.1006/abbi.1997.0356

567 Zulliger, R., Conley, S.M., Naash, M.I., 2015. Non-viral therapeutic approaches to ocular diseases: An
568 overview and future directions. J. Control. Release 219, 471–487.
569 doi:10.1016/j.jconrel.2015.10.007

570